Tree Physiology 33, 135–151
doi:10.1093/treephys/tps118

Research paper

The effects of elevated CO_2 and nitrogen fertilization on stomatal conductance estimated from 11 years of scaled sap flux measurements at Duke FACE

Eric J. Ward[1,2,3,9], Ram Oren[1,4], David M. Bell[1,2], James S. Clark[1,5], Heather R. McCarthy[6], Hyun-Seok Kim[7] and Jean-Christophe Domec[1,3,8]

[1]Nicholas School of the Environment and Earth Sciences, Duke University, Durham, NC 27708, USA; [2]University Program in Ecology, Duke University, Durham, NC 27708, USA; [3]Department of Forestry and Environmental Resources, North Carolina State University, Raleigh, NC 27695, USA; [4]Department of Forest Ecology & Management, Swedish University of Agricultural Sciences (SLU), SE-901 83 Umeå, Sweden; [5]Department of Statistical Science, Duke University, Durham, NC 27708, USA; [6]Department of Botany and Microbiology, University of Oklahoma, Norman, OK 73019, USA; [7]Department of Forest Sciences, College of Agriculture and Life Sciences, Seoul National University, 599 Gwanak-ro Gwanak-gu, Seoul 151-921, Republic of Korea; [8]Bordeaux Sciences AGRO, UMR 1220 TCEM INRA, 1 Cours du général de Gaulle, 33175 Gradignan Cedex, France; [9]Corresponding author (eric.ward@duke.edu)

Received March 30, 2012; accepted November 2, 2012; published online December 13, 2012; handling Editor David Whitehead

In this study, we employ a network of thermal dissipation probes (TDPs) monitoring sap flux density to estimate leaf-specific transpiration (E_L) and stomatal conductance (G_S) in *Pinus taeda* (L.) and *Liquidambar styraciflua* L. exposed to +200 ppm atmospheric CO_2 levels (eCO_2) and nitrogen fertilization. Scaling half-hourly measurements from hundreds of sensors over 11 years, we found that *P. taeda* in eCO_2 intermittently (49% of monthly values) decreased stomatal conductance (G_S) relative to the control, with a mean reduction of 13% in both total E_L and mean daytime G_S. This intermittent response was related to changes in a hydraulic allometry index (A_H), defined as sapwood area per unit leaf area per unit canopy height, which decreased a mean of 15% with eCO_2 over the course of the study, due mostly to a mean 19% increase in leaf area (A_L). In contrast, *L. styraciflua* showed a consistent (76% of monthly values) reduction in G_S with eCO_2 with a total reduction of 32% E_L, 31% G_S and 23% A_H (due to increased A_L per sapwood area). For *L. styraciflua*, like *P. taeda*, the relationship between A_H and G_S at reference conditions suggested a decrease in G_S across the range of A_H. Our findings suggest an indirect structural effect of eCO_2 on G_S in *P. taeda* and a direct leaf level effect in *L. styraciflua*. In the initial year of fertilization, *P. taeda* in both CO_2 treatments, as well as *L. styraciflua* in eCO_2, exhibited higher G_S with N_F than expected from shifts in A_H, suggesting a transient direct effect on G_S. Whether treatment effects on mean leaf-specific G_S are direct or indirect, this paper highlights that long-term treatment effects on G_S are generally reflected in A_H as well.

Keywords: allometry, hierarchical Bayes, hydraulic architecture, Jarvis model, leaf area, *Liquidambar styraciflua*, photosynthetic active radiation, *Pinus taeda*, sapwood area, soil moisture, tree height, vapor pressure deficit.

Introduction

There has now been nearly three decades of active research on the effects of elevated atmospheric carbon dioxide (eCO_2) on tree species (see reviews of Eamus and Jarvis 1989, Mousseau and Saugier 1992, Ceulemans and Mousseau 1994, Gunderson and Wullschleger 1994, Luo et al. 2001, Ainsworth and Long 2005). Among these, early seedling studies led to the view that decreased stomatal conductance (G_S) was a likely response of many species to eCO_2, resulting in decreases in transpiration per unit leaf area (E_L). However, these same studies also

suggested that total canopy leaf area was likely to increase under eCO_2, making uncertain the effect of eCO_2 on total canopy transpiration (Woodward 1990). It remained unclear as to whether such increases in leaf area would be maintained in mature canopies or simply represented accelerated ontogeny (Gunderson and Wullschleger 1994). Interactions of eCO_2 effects with water stress, nutrient limitations and other factors important to tree growth in the field also remained uncertain. To investigate such questions, long-term experiments were conducted with the use of open top chambers (Curtis and Teeri 1992, Norby et al. 1992, 1999, Zak et al. 1993, Ceulemans et al. 1995, Thiec et al. 1995, Pataki et al. 1998) and later, free-air CO_2 enrichment (FACE). A prototype FACE system (Lewin et al. 1992, Hendrey and Kimball 1994, Hendrey et al. 1999) for mature trees began operation in Duke Forest, NC, USA in 1994, followed by a replicated study from August 1996 until October 2010. In this paper we examined an 11-year data set (1998–2008) on E_L and G_S of the major canopy species, loblolly pine (*Pinus taeda* L.) and the co-dominant hardwood, sweetgum (*Liquidambar styraciflua* L.), at this site.

It was noted in early studies of many species that there was a direct leaf-level effect of eCO_2 decreasing G_S in many tree species (Eamus and Jarvis 1989, Will and Teskey 1997). However, in the study of field-grown trees, it was noted that long-term eCO_2 exposure in conifers resulted in small or non-significant decreases in G_S, in contrast to woody deciduous and herbaceous plants (Saxe et al. 1998, Medlyn et al. 2001). While a meta-analysis of FACE studies suggested that trees generally respond to eCO_2 by reducing G_S (Ainsworth and Rogers 2007), *P. taeda* guard cells have been noted to be unresponsive to eCO_2 in porometry studies, except in newly emerged needles (Ellsworth et al. 2011).

In the absence of such a direct effect of eCO_2 on G_S, there may still be an indirect effect through changes in tree structure affecting the distribution of light in the canopy and the hydraulic supply of water to leaves. Increases in leaf area of a canopy will increase shading, leading to lower leaf-specific photosynthetic rates, which would expect to be accompanied by lower G_S in this species (Will and Teskey 1997). As the hydraulic supply is a plastic characteristic of trees in the long term (Mencuccini 2003), it may exhibit adaptations that reinforce changes in light availability leading to decreases in G_S after multiple seasons of exposure to eCO_2. We can represent the hydraulic supply of water for transpiration (Shinozaki et al. 1964, Jarvis 1975, Whitehead and Jarvis 1981, Waring et al. 1982, Whitehead et al. 1984, Tyree and Ewers 1991, Whitehead 1998) as:

$$G_S D \propto k_\Psi \Delta\Psi \frac{A_S}{A_L h} = k_\Psi \Delta\Psi A_H, \quad (1)$$

where transpirational demand is proportional to G_S times the vapor pressure deficit (D). The hydraulic conductivity (k_Ψ) of sapwood as a function of water potential, the difference in soil and leaf water potentials ($\Delta\Psi$) and the hydraulic allometry of trees (A_H) represent three factors that could respond to eCO_2 treatments. This last component can be indexed by the sapwood area (A_S), supplying a distal leaf area (A_L) as representative values for the entire path length of water, approximated by mean tree height (h). At Duke FACE across a wide range of soil moistures, differences have not been detected between treatments in pre-dawn and midday water potential of leaves of *P. taeda*, suggesting similar $\Delta\Psi$ in all treatments for the main canopy species (Domec et al. 2009*b*). This leaves the possibility that indirect effects of eCO_2 on G_S in this species could occur through changes in k_Ψ and/or A_H at this site.

In this study, we examine a network of TDPs monitoring sap flux density and scale these data to estimates of leaf-level E_L and G_S in *P. taeda* and *L. styraciflua* exposed to eCO_2 levels and nitrogen fertilization (N_F). Studies employing TDPs offer an advantage over porometry by integrating over a much larger leaf area and allowing measurements under conditions that make porometric estimates of G_S difficult, such as low soil and leaf water potentials associated with long- and short-term water stress. One study at this study site (Schäfer et al. 2002) noted that *P. taeda* under eCO_2 only reduced stomatal conductance with extreme drought, which was rare during that study period. Conversely, a later study suggested that *P. taeda* under eCO_2 only reduced stomatal conductance at high soil moisture (Domec et al. 2009*b*), in part linked to changes in A_H. We undertook the examination of an 11-year period for which there are well-replicated sap flux and allometric data at this site to examine the effects of eCO_2 and N_F on G_S at this site.

In order to assess differences between treatments, we sought an approach that could aggregate the uncertainty associated with multiple sources of error that enter in long-term studies employing TDPs. Thermal dissipation probes are a widely employed technique for estimating forest water use (Swanson 1972, Swanson and Whitfield 1981, Granier 1987, Smith and Allen 1996, Loustau et al. 1998, Wullschleger et al. 1998, Oren et al. 1999, Lu et al. 2004). Scaling TDP measurements to trees or stands requires information about the variation of flux rates with tree size and radial position in sapwood (Phillips et al. 1996, Oren et al. 1998, Schäfer et al. 2002, Ford et al. 2004). Sensor failures also necessitate users of TDPs to deal with missing observations in long-term studies. To produce a continuous estimate of transpiration, many users fill resulting gaps in data with regressions of broken sensors against working ones or with relationships to environmental drivers, creating a source of unknown errors in these estimates. We estimate these errors in a hierarchical Bayes state-space framework that uses the temporal structure of data to accommodate missing values (Clark et al. 2011).

Using such a model, we assessed the stomatal behavior of *P. taeda* and *L. styraciflua* over a period of 11 years at the

half-hourly time step, with a data set of nearly 20,000 time steps and millions of individual data points. In doing so, the variability across many TDPs was used to not only provide a confidence envelope on E_L estimates, but also information on a latent variable of interest (G_S) and its responses to three environmental drivers: vapor pressure deficit (D), incident photosynthetic photon flux density (Q) and soil moisture (M). We examined how these responses changed over seasons and years, and differed between treatments and species. Specifically, we investigated whether each species exhibited differences in mean monthly daytime G_S between treatments and if these were related to differences in the proportional response of G_S to the environmental drivers. We examined if G_S in each species was positively related to the index of hydraulic allometry (A_H) and if this dataset of TDP measurements confirmed past porometry findings of consistently reduced G_S in *L. styraciflua* in eCO_2 (Herrick et al. 2004).

Materials and methods

Data collection

We used data collected from 1998 to 2008 at the Duke FACE facility in a *P. taeda* plantation established from 3-year-old seedlings in 1983. Treatments included eCO_2 (200 ppm above ambient) using FACE technology on 30-m diameter plots (Hendrey et al. 1999), as well as nitrogen fertilization (N_F, 11.2 g of N m^{-2} $year^{-1}$) in split plots of the CO_2 treatment (Oren et al. 2001). This creates four treatment combinations: ambient CO_2 unfertilized (AC), eCO_2 unfertilized (EC), ambient CO_2 with N_F (AF) and eCO_2 with N_F (EF). The eCO_2 treatment was established in 1994 in a prototype plot with an un-instrumented paired control plot and in 1996 in three additional plots, each with a fully instrumented paired control. The N_F treatment expanded to include 1998 in the prototype and its control and was replicated in 2005 in the other plots. Further details of the site can be found at http://face.env.duke.edu.

Sap flux was monitored at multiple sapwood depths by the use of TDPs constructed in the laboratory (Granier 1987). The number of sap flux sensors for each treatment, species, depth and year is given in the Supplementary Material (see Table S1 available as Supplementary Data at *Tree Physiology* Online). Not all sensors functioned in all months and many sensors were replaced each year due to failures and malfunctions. When a sensor was replaced, the new sensor was placed in the same tree at least 100 mm from the original position. As a sensor in a new location, even when in the same tree, cannot be expected to give the same readings as the previous sensor due to variation in sapwood conductivity (Tateishi et al. 2008), it was treated as a separate sensor for all analyses described below. Thus, the effective number of sensors in the analysis for each time period varied depending on the number of malfunctions and replacements.

To account for night-time conductance, differential voltage data from TDPs were converted to sap flux density values using baseline values established on nights with little to no potential transpiration (Oishi et al. 2008). We used the original 20-mm design and calibration for TDPs (Granier 1987), which was validated for two gymnosperm and one ring-porous angiosperm species (Granier 1985) and later confirmed to be within 15% of flow values within the range of field observations for several other species and porous synthetic materials (Lu et al. 2004). More recently, this calibration has been found to perform well in some diffuse porous species, but under-estimate J_S in ring-porous species and other diffuse porous species (Taneda and Sperry 2008, Bush et al. 2010, Steppe et al. 2010). Long-term deployment and wounding effects have been shown to also affect the accuracy of TDPs (Moore et al. 2010, Wullschleger et al. 2011). Some of these concerns are ameliorated in this study by the large number of sensors (to the extent that errors are random and not biased), the lack of ring-porous species, and the comparisons of each species by treatment (to the extent that trees within a species are equally affected by any bias). We would also note that such errors, once their structure and magnitude are identified, could be accommodated by modifications to the data model in the approach below, which now assumes individual random effects for each sensor to accommodate these many possible sources of error.

Environmental covariates measured at the site included air temperature (T, °C) and vapor pressure deficit (D, kPa) at 2/3 canopy height in each plot (HMP series, Campbell Science, Logan, UT, USA), volumetric soil moisture content from 0 to 0.3 m depths (M, cm^3 cm^{-3} soil) measured at four points in each of the eight plots (CS615 & CS616L, Campbell Science) and the incident photosynthetic photon flux density (Q, mmol m^{-2} ground s^{-1}) at the top of the canopy (LI-190, Li-Cor Biosciences, Lincoln, NE, USA). Data were logged at 30 s intervals and half-hourly averages were recorded using a data logger in each plot (CR-23x, Campbell Science).

Annual surveys of the diameter of all trees >2 cm were conducted and used for the determination of sapwood area. A height survey was conducted with laser range finders in 2002, then yearly with crown length surveys from 2005 to 2008. Annual heights were then interpolated with relationships to diameter at breast height (DBH) (McCarthy et al. 2010). *Pinus taeda* had little to no heartwood formation when harvested in 2011 (P. Torngern, personal communication), so the sapwood area of each tree was taken as the basal area minus the bark thickness. The sapwood area of *L. styraciflua* was calculated from DBH as 0.82 times the basal area (K.V.R. Schäfer, unpublished data). Heights and sapwood areas were all linearly interpolated to daily values. Daily leaf area was determined following the procedure outlined in McCarthy et al. (2007).

Model structure and simulation

In this section we will describe the dynamic empirical model for stomatal conductance (G_S) driven by vapor pressure deficit (D), volumetric soil moisture (M) and photosynthetic photon flux density (Q), followed by a description of how this is scaled to leaf-specific transpiration (E_L) and sap flux at individual sensor locations (J_S). All abbreviations and indices for model components are given in Table 1. A full model description is given in Bell (2011). A hydraulic model (Ward et al. in review) was used to scale E_L to mean sap flux for each species, but is not presented here for brevity. The following section will discuss posterior simulation of model parameters and error, i.e., how the model was fitted to data, while the focus of this section is the description of responses that are of physiological interest. It should be noted this numerical posterior simulation requires a model that describes the processes generating the data to be described (J_S), so this model description starts with the process of interest (G_S), then describes how this is translated to transpiration (E_L) and, finally, J_S. This is the opposite of most descriptions of sap flux studies, but the end result is similar: an estimate of G_S and its responses to environmental drivers conditioned on J_S data across many sensors. This model was used to estimate half-hourly values of J_S for hundreds of sensors over 11 years (see Supplementary Material, Table S1 available as Supplementary Data at *Tree Physiology* Online), for a total of more than 36 million values, representing one of the largest analyses of sap flux data at a single site to date.

Similar to the approach of Jarvis (1976), we modeled canopy-averaged steady-state stomatal conductance (G_{SS}) of each species s in treatment j at time t as a function of the responses to vapor pressure deficit (f_D), volumetric soil moisture (f_M) and photosynthetic photon flux density (f_Q), relative to a reference conductance (G_{SRef}):

$$G_{SS(jst)} = G_{SRef(js)} f_{D(jst)} f_{M(jst)} f_{Q(jst)}, \quad (2)$$

where $f_{D(jst)} = (1 - \lambda_{(js)} \ln (D_{(jst)}))$, while both $f_{M(jst)}$ and $f_{Q(jst)}$ vary positively 0 to 1, making $G_{SRef(js)}$ an index of G_S at high Q, high M and 1 kPa D (Oren et al. 1999). Unlike a theoretical maximum G_S (Jarvis 1976, Oren et al. 1999), this definition of G_{SRef} has the advantage of being within a range of D where estimates are precise enough for the estimation of G_S from sap flux (Ewers and Oren 2000). As f_D approaches infinity at zero D, it does require the specification of a maximum G_S, which we took to be $G_{SRef} + 2\lambda G_{SRef}$. The response to Q was taken as

$$f_{Q(jst)} = 1 - \beta_{1(js)} \exp\left(\frac{-Q_{(t)}}{\beta_{2(js)}}\right), \quad (3)$$

where $1 - \beta_1$ is the ratio of G_S at zero Q to the maximum (thus allowing for night-time conductance) and β_2 is the value of Q at which f_Q is 63% of its maximum. The response to M was taken to be a piecewise function:

$$\begin{cases} f_{M(jst)} = \exp\left(-0.5\left(\dfrac{M - \beta_{4(js)}}{\beta_{3(js)}}\right)^2\right) & \text{for } M < \beta_{4(js)} \\ f_{M(jst)} = 1 & \text{for } M \geq \beta_{4(js)} \end{cases}, \quad (4)$$

where β_4 is the threshold M below which G_S decreases and β_3 controls the rate of this decrease.

It is assumed that there is a stomatal time constant ($\tau = 20$ min for both species) for the response of G_S to changing conditions, i.e., there is no instantaneous adjustment to a steady-state conductance G_{SS} calculated according to Eq. (3). Thus, the time series of G_S is modeled at each time step ($dt = 30$ min) as (Rayment et al. 2000)

$$G_{S(jst)} = G_{S(js(t-dt))} + (G_{SS(jst)} - G_{S(js(t-dt))})\left(1 - \exp\left(\frac{-dt}{\tau_{(js)}}\right)\right), \quad (5)$$

where dt is 30 min. This stomatal time constant has been shown to range from 15 to 50 min for responses to changes in leaf irradiance in *P. taeda* (Whitehead and Teskey 1995).

Canopy-averaged conductance was converted from mmol m^{-2} s^{-1} to kg m^{-2} s^{-1} after Pearcy et al. (1989) scaled to leaf-specific transpiration ($E_{L(jst)}$) for each species as $G_{S(jst)} = c_{(t)} E_{L(jst)}/D_{(t)}$, where $c_{(t)} = 115.8 + 0.4226\ T_{(t)}$ is a conductance constant (kPa m^3 kg^{-1}), estimated from the combined temperature sensitivities of latent heat of vaporization, density of air and psychrometric constant (Phillips and Oren 1998). This simplified calculation assumes that boundary-layer conductance greatly exceeds G_S. For *P. taeda* at this site, Domec et al. (2009*b*) estimated mean daytime boundary-layer conductance to be ~65 times G_S, but this may represent a source of error for *L. styraciflua*, which has larger leaf dimensions. Leaf-specific transpiration is multiplied by leaf area ($A_{L(jst)}$) and divided by total sapwood area ($A_{S(jst)}$) for the species to obtain mean sap flux across all sapwood area for the species ($\overline{J_{S(jst)}}$), after accounting for a hydraulic time constant (κ) using a simple hydraulic model (Ward et al. in review). The sap flux measured by each sensor ($J_{S(jstdi)}$) was then estimated from $\overline{J_{S(jst)}}$ by multiplication with a random effect for each sensor $\phi_{(jstd)}$. To preserve the total amount of sap flux in balance with transpiration (after accounting for changes in water storage), we constrained the mean random effect ($\overline{\phi_{(jstd)}}$) of sensors at each of n depth ranges (d, see Table 1) so that:

$$\sum_{d=1}^{n} \frac{A_{S(jstd)} \overline{\phi_{(jstd)}}}{\sum_{d=1}^{n} A_{S(jstd)}} = 1. \quad (6)$$

Table 1. Abbreviations. Model components have indices for sensor *i* at depth *d* at time *t* for species *s* in treatment *j* or some subset of these.

Abbreviations for model components		Units
$A_{L(jst)}$	Leaf area per unit ground area (leaf area index)	Ratio
$A_{S(jstd)}$	Sapwood area per unit ground area	$mm^2\ m^{-2}$
$c_{(t)}$	Conductance coefficient at temperature *T*	kPa
$D_{(t)}$	Vapor pressure deficit at 2/3 canopy height	kPa
$E_{L(jst)}$	Canopy-averaged transpiration per unit leaf area	$kg\ m^{-2}$
$f_{D(jst)}$	Proportional response of G_S to *D*	Ratio
$f_{M(jst)}$	Proportional response of G_S to *M*	Ratio
$f_{Q(jst)}$	Proportional response of G_S to *Q*	Ratio
$G_{S(jst)}$	Canopy-averaged stomatal conductance per unit leaf area	$mmol\ m^{-2}\ s^{-1}$
$G_{MAX(t)}$	Maximum G_S	$mmol\ m^{-2}\ s^{-1}$
$G_{SRef(js)}$	Reference G_S at 1 kPa *D*, saturating *M* and *Q*	$mmol\ m^{-2}\ s^{-1}$
$G_{SS(jst)}$	Steady state G^S from Eq. 2	$mmol\ m^{-2}\ s^{-1}$
$J_{S(jstdi)}$	Sap flux density per unit sapwood area	$g\ m^{-2}\ s^{-1}$
$M_{(jt)}$	Volumetric soil moisture at 0–30 cm depth	Ratio
$Q_{(t)}$	Incident photosynthetic photon flux density	$mol\ m^{-2}\ s^{-1}$
$T_{(t)}$	Air temperature at 2/3 canopy height	°C
$V_{\tau(js)}$	Scaling factor for G_S dynamics and error from τ	Ratio
$\beta_{1(js)}$	Ratio of G_{SS} at night to G_{SS} at saturating *Q*	Ratio
$\beta_{2(js)}$	*Q* at which $f_Q = 0.63$	$mol\ m^{-2}\ s^{-1}$
$\beta_{3(js)}$	Sensitivity of G_S to *M* below β^4	Ratio
$\beta_{4(js)}$	*M* above which $f_M = 1$	Ratio
$\kappa_{(js)}$	Hydraulic time constant of sap flux at breast height	min
$\lambda_{(js)}$	Sensitivity of G_{SS} to *D*	$log(kPa)^{-1}$
$\tau_{(js)}$	Stomatal time constant	min
$\rho_{(js)}$	Data error standard deviation	$g\ m^{-2}\ s^{-1}$
$\sigma_{(js)}$	Process error standard deviation	$mmol\ m^{-2}\ s^{-1}$
$\varphi_{(jstdi)}$	Random effect for sensor *i*	Ratio
$\omega_{(js)}$	Standard deviation of φ	Ratio
Other abbreviations		
AC	Ambient CO_2 unfertilized treatment plots	
AF	Ambient CO_2 fertilized treatment plots	
BIC	Bayesian information criterion	
A_H	Allometric scaling of hydraulic pathway	$mm^2\ m^{-3}$
eCO_2	Elevated carbon dioxide treatment	
DOY	Day of year	
EC	Elevated CO_2 unfertilized treatment plots	
EF	Elevated CO_2 fertilized treatment plots	
FACE	Free-air carbon dioxide enrichment	
H	Mean tree height	m
k_Ψ	Specific conductivity of sapwood	$m^2\ MPa^{-1}\ s^{-1}$
N_F	Nitrogen fertilization treatment	
P	Precipitation	mm
TDP	Thermal dissipation probe	
$\Delta\Psi$	Soil-to-leaf water potential difference	MPa

A Gibbs sampling Markov chain Monte Carlo algorithm (Gelfand and Smith 1990) was used to simulate posterior distributions. A complete description of this algorithm, including diagnostics and convergence analyses, is given in Bell (2011). Details specific to this simulation are given in Supplementary Material available as Supplementary Data at *Tree Physiology* Online, including prior and posterior distributions of fit parameters. To account for phenological changes in the evergreen canopy (McCarthy et al. 2006, 2007), we independently simulated posteriors of the data for *P. taeda* for three overlapping intervals per year, corresponding to day-of-year (DOY) intervals (0,146), (110,256) and (219,365) or (219,366) in leap years. These intervals represent periods of low ('spring'), increasing ('growing season') and decreasing ('autumn') A_L, respectively.

All analyses were conducted using Team RDC (2009). A study with dozens of trees with nearly 20,000 half-hourly time steps, leading to millions of individual data points, requires aggregation of model outputs. To evaluate the effect of eCO_2 on G_S for each month of the study, monthly daytime means of G_S and its standard deviation for the elevated treatment (EC/EF) and the corresponding ambient treatment (AC/AF) were used for 10^6 samples of a non-parametric bootstrap. The same procedure was performed for the N_F treatments for data from 2005 to 2008. In comparisons of G_{SRef} and monthly mean daytime values of the product of environmental sensitivities ($f_D f_M f_Q$) between treatments, we employed the *lm* function and the *slope.test* function of the *smatr* package (Warton and Ormerod 2007). In model selection for comparisons of $f_D f_M f_Q$ and mean monthly *M*, as well as seasonal relationships of A_H and G_{SRef}, we chose the model that minimized the Bayesian information criterion (BIC), calculated with *lm* and the BIC function of the *qpcR* package (Ritz and Spiess 2008).

Results

Temporal patterns

The study period included a wide range of environmental conditions (Figure 1). These included wet growing seasons (e.g., 2006) typified by monthly mean daytime vapor pressure deficits (*D*) of ~1 kPa and volumetric soil moistures (*M*) with minimum monthly averages around 0.17–0.20, as well as dry growing seasons (e.g., 2007) typified by mean monthly *D* of 1.5–2.2 kPa and *M* below 0.17 for multiple months. Punctuating these long-term variations in conditions were three major storms: Hurricane Floyd, Hurricane Isabel and an ice storm in December 2002 that caused widespread damage to forests in the region (McCarthy et al. 2007), the effects of which can be seen in the decreases in leaf area (Figure 2), as well as mortality losses and decreased expansion of sapwood area of the two study species (Figure 3). Values are given for fertilization treatments (N_F) before 2005; these are each based on a single split-plot (the FACE prototype and its reference plot) and are not directly comparable to the unfertilized values.

The index of hydraulic allometry, taken as sapwood area divided by the product of leaf area and mean tree height (A_H, $cm^2\ m^{-3}$, Eq. (1)), initially decreased in *P. taeda* as leaf

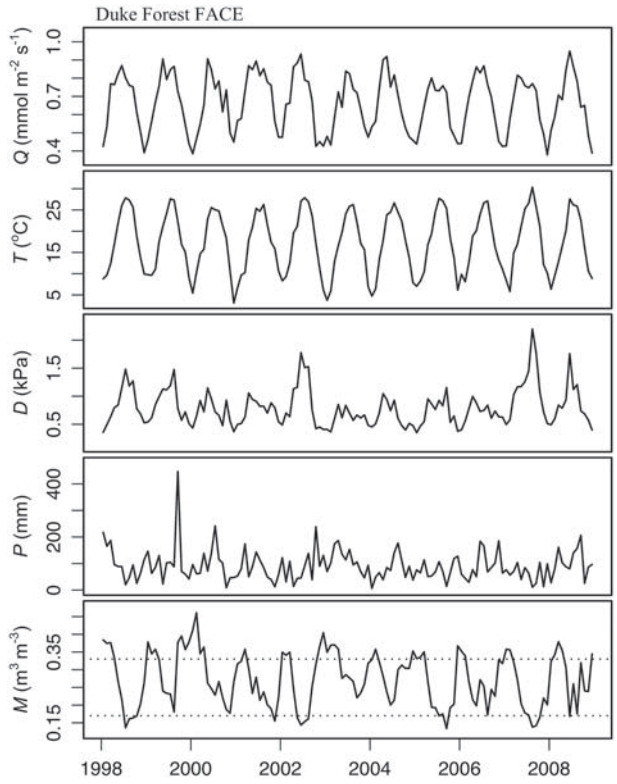

Figure 1. Monthly daytime-averaged environmental covariates for the study period: incident photosynthetic photon flux density (Q), canopy air temperature (T), vapor pressure deficit (D) and volumetric soil moisture content (M), as well as monthly sums of precipitation (P). Dotted horizontal lines represent soil moisture of 0.33 and 0.17, which roughly correspond with field capacity and plant water stress in this soil.

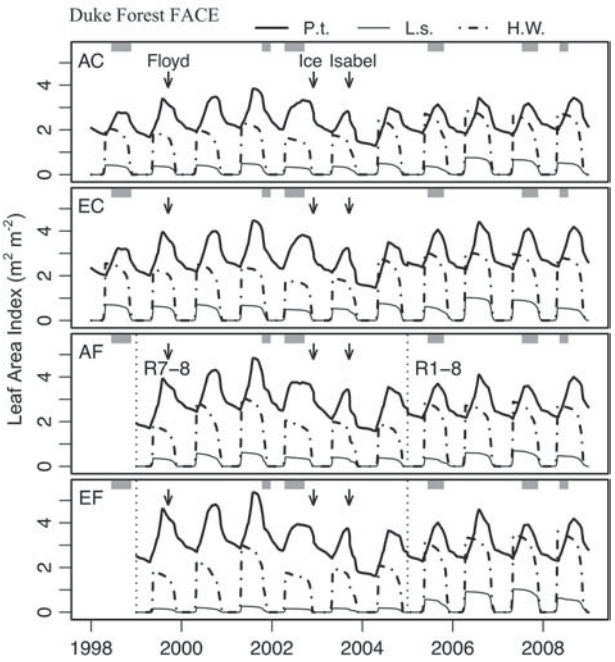

Figure 2. Time courses of leaf area index. *P. taeda* is shown as a solid bold line, *L. styraciflua* as a light solid line and all hardwoods by a dashed line. Drought months (mean volumetric soil moisture <0.17) are indicated by horizontal gray lines at the top of the figure. Major storms causing large canopy disturbances are indicated by name and arrow (see the text). Initial fertilization dates for different FACE plots are indicated with dotted vertical lines. Treatments: ambient CO_2-unfertilized (AC), elevated CO_2-unfertilized (EC), ambient CO_2-fertilized (AF) and elevated CO_2-fertilized (EF). Initial fertilization dates for different FACE plots are indicated with dotted vertical lines.

area and height increased, and then increased with this series of disturbances (Figure 3). In *P. taeda*, A_H was reduced 11–20% with eCO_2, with a mean reduction of 15% over the entire study period, driven mainly by a 19% increase in A_L (Figure 2). In *L. styraciflua*, A_H was reduced 10–39% with eCO_2, with a mean reduction of 23% over the entire study period, resulting from a mean 18% increase in A_L per unit A_S in May–September of each year. Total canopy leaf area recovered by 2005, with a shift towards slightly greater proportion of hardwood leaf area (peak: 50–60%) than before the disturbance (peak: 40–50%) in both treatments. In the period following this recovery, leaf area and A_H followed a more stable annual cycle. This coincided with the replication of the N_F treatment that had been applied to a single plot pair in 1999, which decreased A_H by 8% and increased A_L by 16% in *P. taeda*, while decreasing A_H by 14% and increasing A_L by 26% in combination with eCO_2. In *L. styraciflua*, decreases of 24 and 47% in A_H and increases of 33 and 73% in A_L per unit A_S (in May–September) were observed with N_F and the combined treatment, respectively.

In Figure 4, we present quarterly sums of transpiration per unit leaf area (E_L) and daytime averages of canopy-averaged stomatal conductance (G_S). The general trend for *P. taeda* is a decrease in G_S and E_L during the years 1998–2001, as maximum leaf area (A_L) was increasing, followed by an increase in the years 2002–04 when A_L was decreased by the succession of drought and storms. Of note is the expected drop in G_S during the drought periods indicated by the gray bars, which are the main source of variation in the period with replicated N_F treatments (2005–08). In some years (e.g., 2000), there were large differences in G_S of *L. styraciflua* in different treatments. In other years (e.g., 2001) there was little difference between treatments. The seasonal dynamics showed that little transpiration occurred in the first quarter of each year for this species, so we omitted the G_S values for this mostly leafless period from further analyses.

The effects of the eCO_2 treatment on monthly daytime means of G_S of each species in each fertilization treatment are presented in Figure 5. Lower G_S for *P. taeda* was observed in 65 out of 132 months of study (49%) in unfertilized plots, but not consistently throughout the study period (mean reduction 13%). In the period after replication of the N_F treatments (2005–08), decreased G_S with eCO_2 was detected only in 2 of 48 months in the N_F plots, versus 7 months when G_S was higher with eCO_2 in the N_F plots. In the period before replication of the N_F plots (2001–04), decreased G_S with eCO_2 was

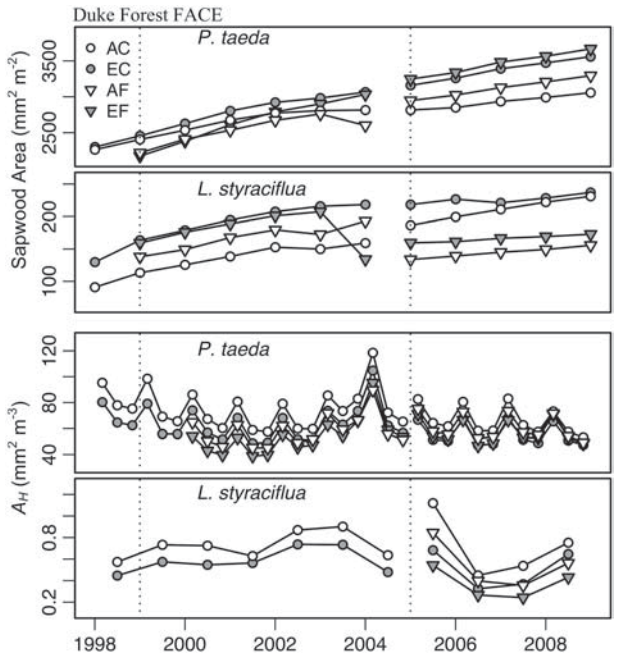

Figure 3. (Upper two panels) Sapwood area per unit ground area of *P. taeda* and *L. styraciflua* (A_S) for AC (open circles), EC (filled circles), AF (open triangles) and EF (filled triangles) treatments. (Lower two panels) Hydraulic allometry (A_H) for each model period for each species, calculated as mean sapwood area per unit leaf area per unit canopy height. Treatments: ambient CO_2-unfertilized (AC), elevated CO_2-unfertilized (EC), ambient CO_2-fertilized (AF) and elevated CO_2-fertilized (EF). Initial fertilization dates for different FACE plots are indicated with dotted vertical lines.

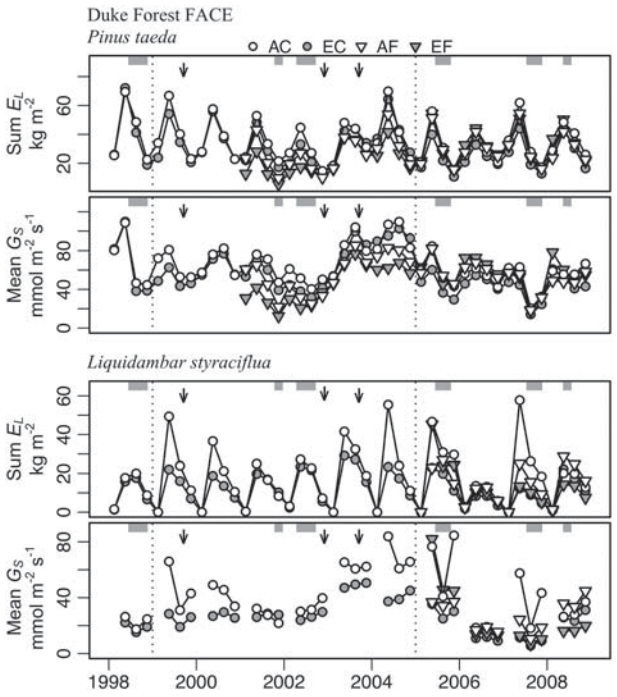

Figure 4. Quarterly sums of transpiration (E_L, leaf-area basis) and mean daytime stomatal conductance (G_S, leaf area basis) estimated from scaled sap flux measurements for *P. taeda* and *L. styraciflua*. The addition of fertilization plots in FACE rings 1–6 is indicated with a dotted vertical line. Drought months and major storms are identified with gray bars and arrows, respectively. Treatments: ambient CO_2-unfertilized (AC), elevated CO_2-unfertilized (EC), ambient CO_2-fertilized (AF) and elevated CO_2-fertilized (EF). Initial fertilization dates for different FACE plots are indicated with dotted vertical lines.

detected in 24 of 48 months in the fertilized plots, with a mean reduction of 22% across the period. The mean daytime G_S was lower in eCO_2 in *L. styraciflua* for 42 of 55 months with stable leaf area (May–September) in unfertilized plots (mean reduction 31%). Results were similar under N_F, except for the initial period following fertilization in 2005 when eCO_2 resulted in higher G_S, followed by a mean reduction of 39% in 2006–08.

Fertilization effects on the monthly daytime means of G_S of each species in each CO_2 treatment are presented in Figure 6, with the fertilized/unfertilized ratio of the hydraulic allometry index (A_H), for the period after replication of the N_F treatments (2005–08). We observed fertilized/unfertilized ratios of A_H below one for *P. taeda* in the ambient CO_2 plots throughout this period. Stomatal conductance remained similar in the ambient CO_2 plots until early 2008, when the N_F treatment began to exhibit lower G_S. In the eCO_2 treatment, A_H of *P. taeda* remained the same or increased slightly, while G_S was increased with N_F in almost all months. For *L. styraciflua*, N_F resulted in lower A_H in both CO_2 treatments, but did not have a consistent effect on G_S in either CO_2 treatment. Due to the large transitional departures between treatments in *L. styraciflua* in 2005 (Figures 5 and 6), this year was omitted from the subsequent analyses of stomatal conductance for this species.

While collinearity of environmental covariates makes univariate responses and their parameters difficult to interpret (see Figure 9, below), the reference conductance, G_{SRef}, and the proportional sensitivity to $D(\lambda)$ represent standard points of comparison to other modeling approaches applied to similar data sets (Figure 7). For *P. taeda*, G_{SRef} ranged from ~50 to 150 mmol m^{-2} s^{-1}, with a similar temporal trend as noted for G_S in Figure 4. On the other hand, λ had spring values almost all near the minimum of 0.45, while mid-growing season values ranged up to 0.75 with considerable yearly variation and autumn values were intermediate between these. While *P. taeda* did not exhibit large differences between treatments in these parameters, *L. styraciflua* did, with G_{SRef} in AC sometimes much higher, and sometimes similar to that in the EC treatment.

The model provides predictions for each sensor for each time period, as well as random effects that can be averaged to describe the radial pattern of sap flux. The most distinct pattern that arose in the data model parameters was a decrease in the ratio of outer to mean sap flux from ~1.4 to ~1.1 in pine

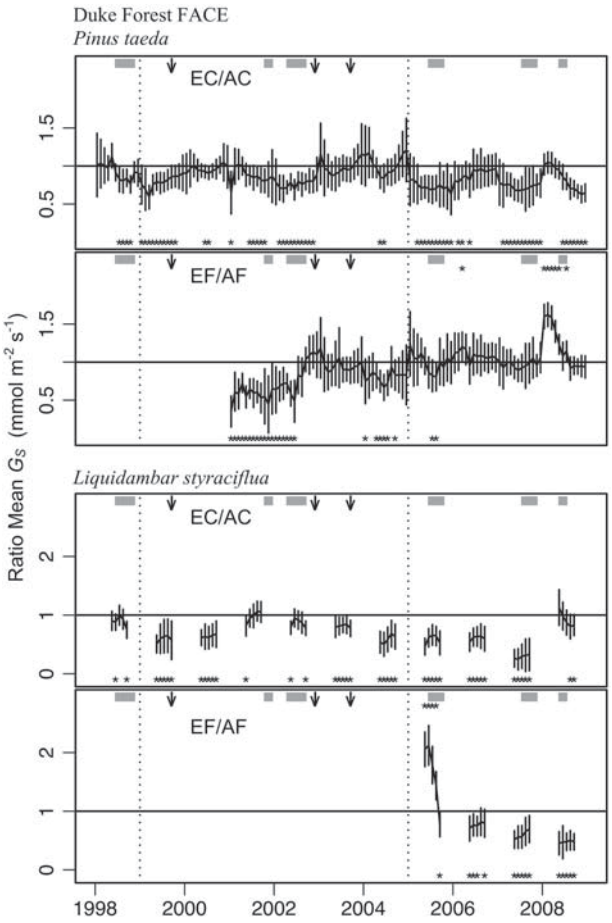

Figure 5. Monthly ratios in mean daytime stomatal conductance (G_S) between elevated and ambient CO_2 plots in unfertilized (EC/AC) and fertilized (EF/AF) treatments. Bars represent the means of the 95% credible interval bounds for each month. Stars denote months where bootstrapped posterior means of elevated treatment were above (top) or below (bottom) ambient values in 95% or more of samples. Drought months and major storms are identified with gray bars and arrows, respectively. Initial fertilization dates for different FACE plots are indicated with dotted vertical lines.

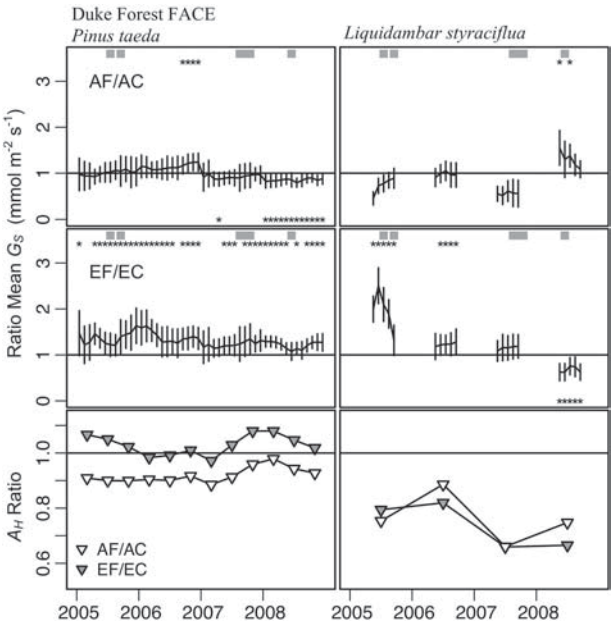

Figure 6. (Upper and middle panels) Monthly ratios in mean daytime stomatal conductance (G_S) between fertilized and unfertilized plots in ambient CO_2 (AF/AC) and elevated CO_2 (EF/EC) treatments. Bars represent the means of the 95% credible interval bounds for each month. Stars denote months where bootstrapped posterior means of fertilized treatment were above (top) or below (bottom) unfertilized treatment values in 95% or more of samples. Drought months are identified with gray bars. (Lower panels) Ratio of hydraulic allometry (A_H) for each model period for each species, calculated as mean sapwood area per unit leaf area per unit canopy height in ambient CO_2 (AF/AC, open triangles) and elevated CO_2 (EF/EC, filled triangles).

trees under eCO_2 following N_F additions in 2005 (EF, Figure 8) as the other treatments increased their ratios to 1.5–1.9. In general, the sap flux profile was flatter in the sweetgum trees, where no consistent pattern by treatment was discernible over this period.

Stomatal responses to environmental drivers

Examining the response of stomata to a single environmental driver is not a complete picture of the effects on G_S, as the univariate responses to vapor pressure deficit (f_D), soil moisture (f_M) and photosynthetic photon flux density (f_Q) interact with each other (Eq. (2)) to produce the G_S estimated in Figure 4. The mean daytime f_M and f_Q are correlated with f_D at the monthly time scale in both *P. taeda* ($f_D = 0.78\ f_M + 0.60$, $R^2 = 0.33$; $f_D = -2.06\ f_Q + 2.58$, $R^2 = 0.41$) and *L. styraciflua* ($f_D = 0.56\ f_M + 0.71$, $R^2 = 0.33$; $f_D = -1.25\ f_Q + 2.01$, $R^2 = 0.22$). Thus, the evaluation of the combined response to all three environmental covariates ($f_D f_M f_Q$) is more appropriate than evaluating the univariate responses to each.

For *P. taeda*, the monthly daytime averages of $f_D f_M f_Q$ in the eCO_2, N_F and combined treatments (EC, AF and EF) regressed against that of the ambient control (AC) values show no regular pattern of difference (Figure 9, top right panel), with slopes and intercepts that do not vary significantly from one and zero, respectively (Table 2). Monthly values of $f_D f_M f_Q$ in AC predict very well $f_D f_M f_Q$ in the other treatments ($R^2 = 0.92$–0.95) for *P. taeda*, suggesting that the difference between the treatment estimates of G_S in each season (Figures 5 and 6) is largely explained by differences in G_{SRef} (Figure 9, top left panel), which exhibits less correlation between treatments (Table 2).

For *L. styraciflua*, the relationships of $f_D f_M f_Q$ in the elevated treatments (EC and EF) to that of the control treatment (AC, Figure 9, bottom left panel) have positive intercepts and slopes less than one; however, mean ratios of $f_D f_M f_Q$ remained close to one (Table 2). Monthly values of $f_D f_M f_Q$ in AC were correlated to $f_D f_M f_Q$ in the other treatments almost as much for *L. styraciflua* as *P. taeda* ($R^2 = 0.78$–0.99). On the other hand, G_{SRef} of this species was highly variable, with that of AC poorly correlated to that of the EC ($R^2 = 0.26$) and AF ($R^2 = 0.39$) treatments.

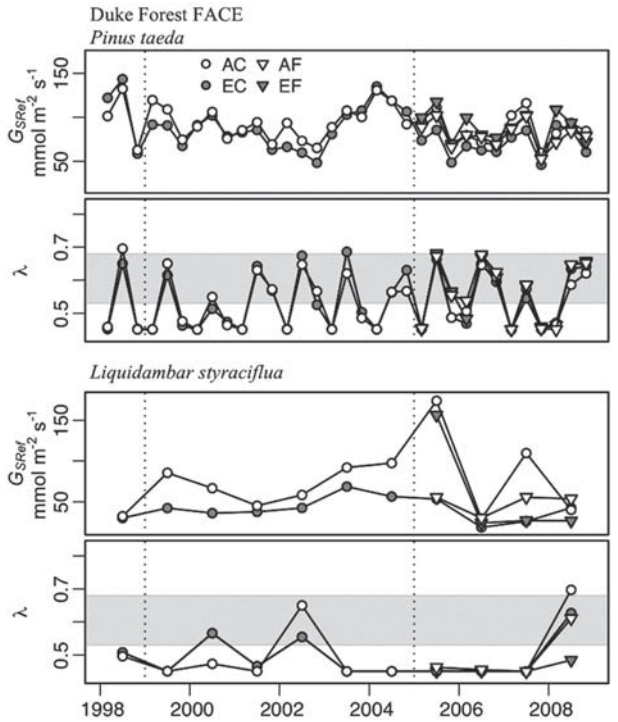

Figure 7. (Top panel) Reference stomatal conductance (G_{SRef}, mmol m^{-2} s^{-1}) of *P. taeda* by model period (three per year). (Second panel) Relative sensitivity (λ) of canopy-averaged stomatal conductance (G_S) to vapor pressure deficit (D) by model period, according to $G_S = G_{SRef}$ $(1 - \lambda \ln(D))$. Gray area is the range of λ values for maximum vapor pressure deficits of 3–5 kPa from Oren et al. 1999. (Bottom panels) Same as above for *L. styraciflua* with one model period per year. Treatments: ambient CO_2-unfertilized (AC), elevated CO_2-unfertilized (EC), ambient CO_2-fertilized (AF) and elevated CO_2-fertilized (EF). Initial fertilization dates for different FACE plots are indicated with dotted vertical lines.

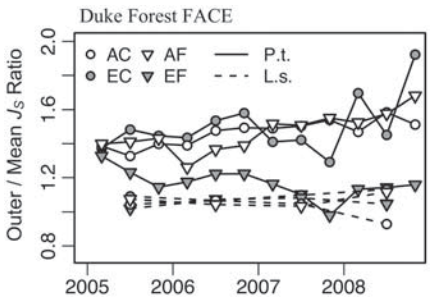

Figure 8. The ratio of outer sap flux (J_S, g m^{-2} s^{-1}) to the mean across all sapwood area by species and treatment for the period after replication of the fertilization treatment. Solid lines connect values for *P. taeda* and dashed lines those for *L. styraciflua*. Treatments: ambient CO_2-unfertilized (AC), elevated CO_2-unfertilized (EC), ambient CO_2-fertilized (AF) and elevated CO_2-fertilized (EF).

While the EF treatment G_{SRef} was correlated to that of AC ($R^2 = 0.76$), the mean ratio was well below one (0.58). This suggests that in this species, as well as *P. taeda*, most of the variability in G_S between treatments is contained within G_{SRef}.

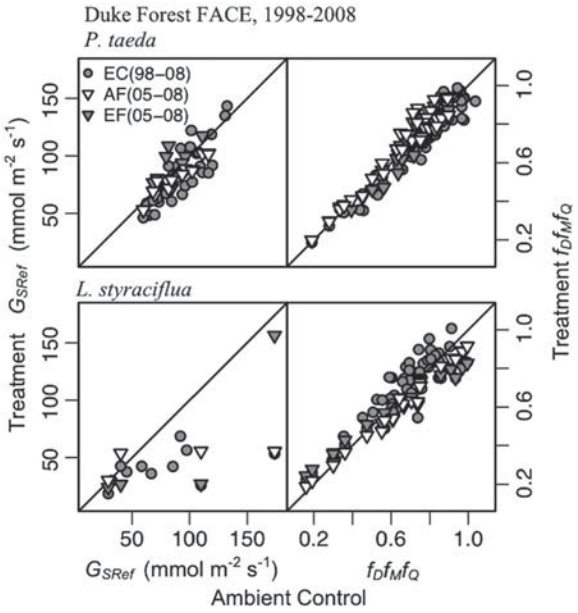

Figure 9. (Left panels) The canopy-averaged stomatal conductance at reference conditions (G_{SRef}) in each treatment versus that of the ambient unfertilized control (AC) for *P. taeda* and *L. styraciflua* for each model period. (Right panels) Monthly daytime means of the combined modeled effect of vapor pressure deficit (f_D), soil moisture (f_M) and photosynthetically active radiation (f_Q) on G_{SRef} for *P. taeda* and *L. styraciflua*. Treatments: ambient CO_2-unfertilized (AC), elevated CO_2-unfertilized (EC), ambient CO_2-fertilized (AF) and elevated CO_2-fertilized (EF). Lines represent a 1 : 1 ratio.

In light of this collinearity of environmental responses, we evaluated the response of each CO_2 treatment to M within each species and fertilization level using monthly average $f_D f_M f_Q$ rather than f_M alone (Figure 10). We estimated this saturating response using a piecewise function, with an initial linear increase estimated from values at monthly average $M < 0.2$ up to a constant value estimated from values at monthly average $M > 0.3$. For each species and fertilization level, we selected the linear model from a set of five nested models with the full model having effects for M and eCO_2, as well as their interaction, and the null model having only an intercept. We selected the model with the lowest BIC value, which was a common linear relationship with M in all cases. Likewise, we found that a constant value for both CO_2 treatments yielded a lower BIC than separate values for the maximum $f_D f_M f_Q$ in all cases. Parameters of these functions are given in Table 3.

Stomatal conductance and hydraulic supply

The relationship between G_{SRef} and the index of hydraulic allometry (A_H, Eq. (1)) for *P. taeda* was steeper during the growing season than the spring and autumn model periods, so we evaluated this relationship separately for the different periods (Figure 11). We also estimated this relationship for *L. styraciflua* (Figure 11, bottom right panel) for the period of each year with active leaf area. This resulted in four species–season

Table 2. Relationships between reference stomatal conductance (G_{SRef}) for each model period, as well as monthly mean proportional response to vapor pressure deficit, light and soil moisture ($f_D f_Q f_M$), for each species in each treatment versus values of ambient CO_2 unfertilized control (AC). Relationships fitted with ordinary least squares have an intercept (b) and a slope (m), with control values as the independent variable. Also given are the coefficient of determination (R^2), P values for F-tests of the null hypotheses $b = 0$ and $m = 1$ and the mean ratios of treatment to control values for 2005–08 for *P. taeda* and 2006–08 for *L. styraciflua*. Treatments: elevated CO_2-unfertilized (EC), ambient CO_2-fertilized (AF) and elevated CO_2-fertilized (EF).

			R^2	b	P ($b = 0$)	m	P ($m = 1$)	Ratio
P. taeda	G_{SRef}	AF	0.90	15.0	0.061	0.75	0.012	0.93
		EC	0.71	–11.9	0.291	1.04	0.743	0.90
		EF	0.56	21.1	0.298	0.78	0.339	1.03
	$f_D f_Q f_M$	AF	0.92	0.030	0.324	0.99	0.748	1.03
		EC	0.92	–0.016	0.426	0.99	0.687	0.97
		EF	0.95	0.000	0.992	0.99	0.831	0.99
L. styraciflua	G_{SRef}	AF	0.39	38.45	0.070	0.116	0.192	0.96
		EC	0.26	28.51	0.007	0.169	<0.001	0.65
		EF	0.73	–14.57	0.735	0.829	0.018	0.58
	$f_D f_Q f_M$	AF	0.99	0.038	0.014	0.876	<0.001	0.96
		EC	0.78	0.152	<0.001	0.798	<0.001	1.04
		EF	0.96	0.160	<0.001	0.692	<0.001	1.00

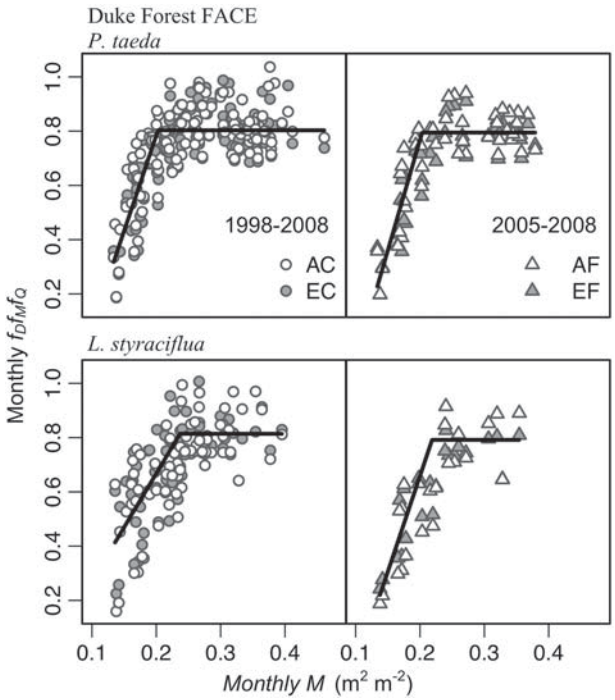

Figure 10. Monthly daytime means of the combined modeled effect of vapor pressure deficit (f_D), soil moisture (f_M) and photosynthetically active radiation (f_Q) on stomatal conductance versus soil moisture (M) for *P. taeda* and *L. styraciflua*. Treatments: ambient CO_2-unfertilized (AC), elevated CO_2-unfertilized (EC), ambient CO_2-fertilized (AF) and elevated CO_2-fertilized (EF). Lines represent a piecewise fit with a linear portion estimated from data below $M = 0.2$ and a constant portion estimated from data above $M = 0.3$.

Table 3. Parameters for piecewise functions in Figure 10 describing relative responses of monthly mean canopy averaged stomatal conductance (G_S) to volumetric soil moisture (M). R^2 values are for linear portion of function using data where M was below 0.2.

Species	Fertilization	Intercept	Slope	Maximum	R^2
P. taeda	Control	–0.623	7.03	0.803	0.59
	N_F	–0.862	8.14	0.795	0.74
L. styraciflua	Control	–0.126	3.97	0.814	0.15
	N_F	–0.754	7.06	0.791	0.64

combinations to be evaluated (Table 4). For each of these, the best-fit of a family of nested models for a linear effect of A_H and factors for eCO_2 and N_F treatments, including all interactions, was selected for each study period as that which minimized BIC (Schwarz 1978). To ease the interpretation of these models, we calculated the expected 2008 values, the end of our study period, 12 years after the initiation of the eCO_2 treatment and 4 years after replication of the N_F treatment.

For *P. taeda*, eCO_2 resulted in slightly higher G_{SRef} during the spring season than would be expected from the changes in A_H alone (Table 4) and a steeper relationship with A_H in the growing season, leading to a similar difference in the range of observations (Figure 11). During autumn, the selected model had a common $A_H - G_{SRef}$ relationship for all treatments for this species. For *L. styraciflua*, we found that the best fit model for the $A_H - G_{SRef}$ relationship had a negative fixed effect for eCO_2, with the predicted 2008 values highest in AC where average A_H was highest.

We have concentrated here on the state-space-modeled process of E_L and G_S. These quantities are direct outputs of the state-space model at the half-hourly time steps, for each of which we can estimate a posterior distribution or some summary statistic of variation (such as a standard deviation), which form the basis of bootstrapped comparisons in Figures 5 and 6. The process error of $\boldsymbol{G}_S$ (σ, mmol m^{-2} s^{-1}) ranged from 2.4 to 20.2 across species, treatments and seasons, with a mean of 10.0 and a median of 6.8, suggesting fairly constrained inference at the canopy level. The posterior estimates of sap

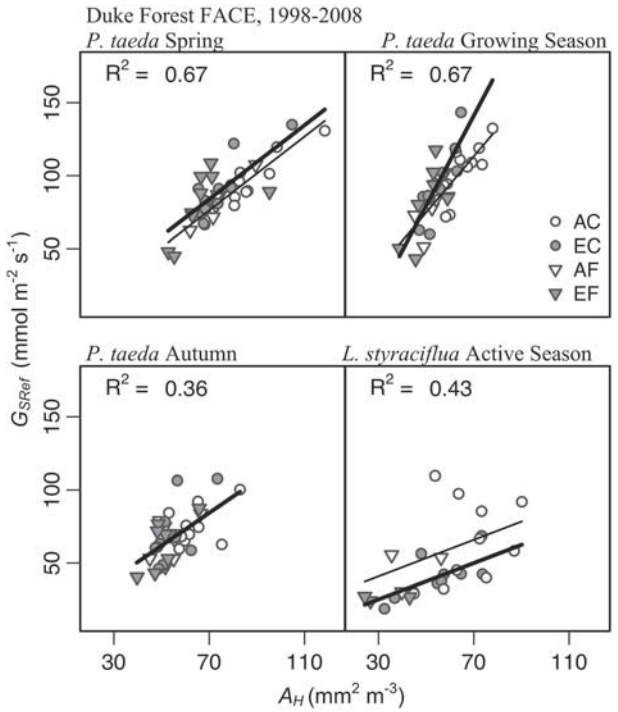

Figure 11. The canopy-averaged stomatal conductance at reference conditions (G_{SRef}) versus hydraulic allometry index (A_H), defined as sapwood area (cm^2) per unit leaf area (m^2) per m canopy height, in each treatment. *Pinus taeda* had three overlapping model periods: spring (DOY <147), growing season (DOY 110–256) and autumn (DOY >218). *Liquidambar styraciflua* had one model period per year defined by the duration of active leaf area. For spring and growing season *P. taeda* values, the bold lines represent elevated CO_2 treatments and the thin lines represent ambient CO_2 treatments. Lines represent effects for a single model selected for each panel and are presented in Table 4. Treatments: ambient CO_2-unfertilized (AC), elevated CO_2-unfertilized (EC), ambient CO_2-fertilized (AF) and elevated CO_2-fertilized (EF).

flux data error ($\rho_{(js)}$, g m^{-2} s^{-1}) ranged from 1.0 to 3.8 across years, treatments and species, with a mean of 2.0 and a median of 1.9, suggesting, with random effects included for individual sensors, that data were generally well predicted by the model.

Discussion

Relationship between A_H and G_S

While our approach allowed us to estimate G_S and associated uncertainty at each half-hour time step, we will discuss an important feature further below, that is, the results of greatest interest are those independent of time. Across the 11-year treatment period, we see that both species had a similar proportional response to environmental drivers in all treatments, with the possible exception of decreased sensitivity to environmental stress in the combined elevated carbon dioxide (eCO_2) and nitrogen fertilization (N_F) treatment for *L. styraciflua* (Figure 9). Thus, the main differences between stomatal responses in different treatments are described well by G_{SRef}. In both species, we found a relationship between the reference stomatal conductance (G_{SRef}) and the hydraulic allometry index (A_H; Figure 11). This pattern has been found in stands across a wide range of biomes (Novick et al. 2009). We cannot conclude from these relationships alone whether any difference between treatments in the stomatal conductance (G_S) inferred from sap flux measurements was driven by direct leaf-level effects or indirect structural effects. Indeed, such effects are not mutually exclusive, as hydraulic allometry is a highly plastic character of most tree species and may be expected to adapt to a long-term decrease in leaf-level G_S (Whitehead et al. 1984, Tyree and Ewers 1991, McDowell et al. 2002, Mencuccini 2002, 2003, Buckley and Roberts 2005). However, if direct leaf-level effects drive differences in G_S, we would expect these differences to exhibit a rapid onset (mean leaf life span or shorter) and persist through changes in A_H, such as canopy disturbances that decrease leaf area.

Effects of eCO_2 and N_F on G_S in P. taeda

In *P. taeda*, we do not find support for a direct effect of eCO_2 on G_S, but rather an indirect effect where decreases in A_H were related to decreases in G_S in some time periods. While the mean G_{SRef} was lower in the EC treatment than in the AC treatment, ~45% of the study period (Figure 5, top panel), we see that it is actually higher than expected based on A_H alone in the spring and growing season (Figure 11, Table 4). A direct leaf-level effect of eCO_2 would be expected to result in more consistent decreases in G_S between these treatments. When canopy leaf area was reduced by a succession of droughts, an ice storm and Hurricane Isabel in 2003 (Figure 2), we failed to detect a difference in G_S with eCO_2 (Figure 5).

The effect of N_F on G_S in *P. taeda* and its interaction with eCO_2 are similarly linked to changes in A_H. We see little evidence of a reduction in G_S with eCO_2 in the N_F treatment after replication in 2005 (Figure 5, second panel). During this period, the mean difference in A_H in AF and EF was 6.1%, versus a difference of 16.1% in AC and EC. The G_S reductions observed in the non-replicated N_F treatments in 2001–02 correspond to a period of canopy disturbance when *P. taeda* A_H in the EF treatment was 21.6% less than that in AF. Fertilization effects on G_S in *P. taeda* differed by CO_2 treatment (Figure 6). In ambient CO_2, N_F decreased A_H an average of 8% from 2005 to 2008. On the other hand, A_H exhibited an average increase of 3% with N_F in the eCO_2 plots. These changes in A_H are consistent with published results from the site that suggested that A_L increases of eCO_2 and N_F were not additive (McCarthy et al. 2007), so that an A_H decrease is driven by increasing A_L in ambient CO_2 (Figure 2) while the A_H increase is driven by increasing A_S in eCO_2 (Figure 3).

Table 4. Relationships between reference stomatal conductance (G_{SRef}, mmol m^{-2} s^{-1}) and sapwood area per unit leaf area divided by the height of the canopy (A_H, mm^2 m^{-3}) for *P. taeda* (*P.t.*) in the spring (Sp, DOY < 147), growing (Gr, DOY 110–256) and autumn seasons (Au, DOY > 218), as well as *L. styraciflua* (*L.s.*) in period of active leaf duration each year. The formula for the best-fit of a family of nested models for a linear effect of A_H and factors for elevated carbon dioxide (eCO_2) and nitrogen fertilization (N_F) is given for each, along with the resulting prediction of G_{SRef} (mmol m^{-2} s^{-1}) at A_H in 2008 for each treatment, Bayes information criterion (BIC) and difference in BIC from a full model with all interactions and a null model with only an intercept. Treatments: ambient CO_2-unfertilized (AC), elevated CO_2-unfertilized (EC), ambient CO_2-fertilized (AF) and elevated CO_2-fertilized (EF).

Species–season	Formula	Predicted 2008 G_{SRef}				BIC	ΔBIC	
		AC	AF	EC	EF		Full	Null
P.t.–Sp	$1.27A_H + 7.8$ $eCO_2 - 12.4$	80	78	78	84	301.9	15.7	34.6
P.t.–Gr	$1.93A_H + 115.6A_H$ $eCO_2 - 53.1$ $eCO_2 - 21.6$	89	82	82	90	242.5	9.6	24.5
P.t.–Au	$1.12A_H + 5.8$	65	61	60	60	310.1	17.6	13.6
L.s.	$0.625A_H - 15.9$ $eCO_2 + 22.2$	69	57	47	33	234.5	15.7	8.0

To the extent that treatment effects represent accelerated ontogeny, we may expect hydraulic limitations to play a large role in structural effects on G_S in *P. taeda*, as stomatal limitation increases and photosynthetic rates decrease with age in stands from 14 to 115 years old (Drake et al. 2010). However, persistent increases of leaf area (A_L) in the treatments after canopy closure (Figure 2) suggest that these effects do not simply arise from accelerated ontogeny. As *P. taeda* saplings grown in eCO_2 exhibited no difference in J_S, G_S or sapwood-to-leaf-area ratios after 4 years of exposure in open top chambers (Pataki et al. 1998), it may be that such indirect effects on G_S are only evident in mature stands with closed canopies after many years of exposure. Such stands have limitations to leaf gas exchange that accompany any increases in hydraulic constraints with increased A_L.

The indirect nature of a structural effect may explain why past studies at this site have not found a consistent decrease of G_S with eCO_2 in *P. taeda*, although it has been suggested that one exists under only low soil moisture (Schäfer et al. 2002), high soil moisture (Domec et al. 2009*b*) or on newly emerged needles (Ellsworth et al. 2011). We do not find a difference between CO_2 treatments in the proportional reduction of G_S as soil moisture declines (Figure 10). Previous estimates of the effect of eCO_2 on whole-tree hydraulic conductivity (Domec et al. 2010) include an increase early in the study (2000) followed by a decrease later in the study (2007). This lag effect of fumigation on G_S in *P. taeda* can be explained by the length of exposure to eCO_2 necessary to affect pre-treatment hydro-active xylem and thus to produce a reduction in whole-tree hydraulic conductivity and consequently G_{SRef}. Our results confirm that G_S of *P. taeda* under eCO_2 was noticeably reduced in 2007 but not 2000 (Figure 4), although these decreases are not simply increasing with time, in part due to fluctuations in A_L (Figure 2) and their effects on A_H (Figure 3).

Effects of eCO_2 and N_F on G_S in L. styraciflua

Unlike *P. taeda*, our analysis of sap flux in *L. styraciflua* is consistent with a direct effect of eCO_2 on G_S in this species. The G_S estimates are lower in EC than in AC for 76% of the months studied, as well as in EF versus AF in 2006–08 (Figure 5, bottom panels). A decrease in G_S with eCO_2 in this species has been inferred from sap flux (Schäfer et al. 2002) and directly observed in a porometry study (Herrick et al. 2004) at this site, as well as another FACE site where it forms the main canopy (Gunderson et al. 2002, Wullschleger et al. 2002, Warren et al. 2011). The lower intercept of the $A_H - G_{SRef}$ relationship of the eCO_2 treatments (Figure 11) is also consistent with a direct effect at the leaf level.

We cannot rule out a change in sapwood conductivity, however. As younger xylem tends to play a greater role in water transport in angiosperms than in conifers, it may also change sapwood conductivity more quickly in response to such treatments. Previous study of sapwood conductivity in this species has found that eCO_2 decreased sensitivity to Ψ in roots, but increased it in branches at this site (Domec et al. 2010), although the effects on stem wood have not been investigated. The difference in G_{SRef} with eCO_2 is accompanied by a drop in A_H, as indicated by predicted differences in G_{SRef} under eCO_2 at the end of the study period that exceed this fixed effect in both fertilization treatments (Table 4). This shift along the $A_H - G_{SRef}$ relationship in this species may reflect adjustment of hydraulic supply to a drop in long-term demand from a direct effect at the leaf level. This may play a role in G_S differences noted in field experiments of the two groups under eCO_2 (Saxe et al. 1998).

Despite large decreases in A_H with N_F in *L. styraciflua*, we do not see a consistent concomitant reduction in G_S (Figure 6). This species is generally situated lower in the canopy than the dominant pines, making A_H less reflective of other canopy structure effects, such as light availability. The common

$A_H - G_{SRef}$ relationship between fertilization treatments may mask underlying differences in components of the hydraulic pathway that warrant further investigation using data from whole-tree harvests. Furthermore, the use of annual values for A_H in this species would mask effects such as the earlier leaf senescence during droughts observed under eCO_2 in this species at the FACE site in Oak Ridge, TN (Warren et al. 2011). However, the fact that we do find a relationship between G_{SRef} and A_H in this species illustrates the balance between the demands of gas exchange and the hydraulic supply of water to the canopy over the long term. It also shows that while we incorporated the expectation of a hydraulic time constant increasing with height in *P. taeda*, such an expectation is not necessary to produce a relationship between G_{SRef} and A_H, as we did not consider hydraulic time constants in *L. styraciflua*.

Seasonal trends in stomatal responses of *P. taeda*

Slopes of the $A_H - G_{SRef}$ relationships are greater in the growing season than in spring or autumn (Table 2) and there were large seasonal fluctuations in estimates of the relative response of G_S to D (λ, Figure 7) for *P. taeda*. While maintaining an evergreen canopy, *P. taeda* only maintains 2 years of needle growth, resulting in large seasonal fluctuations in A_L (Figure 2) and thus A_H (Figure 3). Furthermore, the age structure of this leaf area changes throughout the year, with important functional differences between current- and previous-year needles in both gas exchange (Ellsworth et al. 2011) and hydraulic characteristics (Domec et al. 2009*a*). While we did account for the effect of light availability on G_S (Eq. (3)), the use of incident radiation at the top of the canopy does not account for seasonal changes in sun angle and its effects on light transfer within the canopy of heterogeneously distributed leaf area. A recent Bayesian model starvation analysis (Mackay et al. 2012) has shown that the effects of canopy gaps on light transfer can be crucial for correct estimation of transpiration in simple models. For these and other reasons, it should not be surprising to find such seasonal trends in parameters of our simple model of G_S in this species and we found it prudent to separate analyses by seasons rather than years.

While different ranges of D have been found to affect estimates of λ in linked hydraulic and G_S models (Oren et al. 1999), the seasonal trend in λ (Figure 7) for *P. taeda* does not simply arise from this effect. Indeed, if this were the case, we would expect lower values of λ in the mid-growing season where D exhibits the greatest range; instead we found a trend in the opposite direction. As sensitivities were lowest in the spring period, when A_L reaches its minimum and highest in the growing season when water stress is highest and A_L is increasing, this may represent a seasonal trend in sensitivity linked to A_H that warrants further study.

It could also be that the lower signal-to-noise ratios or lower temperatures in the non-growing seasons make it difficult to resolve λ during these time periods. One may also expect trade-offs between the effects of D and soil moisture (f_D and f_M), which are strongly collinear on the monthly and seasonal time scales in our study ($R^2 = 0.33$ for both species) as well as others (Oishi et al. 2010). This may not be apparent if data are selected by boundary-line analysis before calculating these effects, as in other sap flux studies (Schäfer et al. 2000, Ewers et al. 2001). While we made an effort to separate these effects, the method here differs from boundary-line analysis in that there is no additional step to select the upper range of G_S estimates within bins of D. We may expect that such upper limits are more likely to test the hydraulic capacity of a tree to transport water and thus better match idealized inputs of models such as those used by Oren et al. (1999), whereas the approach here may better reflect the mean responses of a canopy in a dynamically changing environment.

Transient effects of nitrogen fertilization

For both species, there could be an increase in conductance in the first few years following fertilization that deviates from the expected $A_H - G_{SRef}$ relationship (Table 4), due to increases in photosynthetic rate (Murthy et al. 1996, Maier et al. 2008), and thus G_S, that may decrease with time after initial fertilization (Gough et al. 2004). For *P. taeda* in both CO_2 treatments, G_S with N_F in 2005–06 was much greater than expected from the $A_H - G_{SRef}$ relationships (Table 4). There was no detectable decrease in G_S with N_F in the ambient CO_2 during this time (Figure 6), when the predicted values would be decreases of 6–12%, depending on season. Under eCO_2, there was a 37% mean increase in G_S, where the expectation would be between a 9% decrease and a 2% increase, depending on season. The temporary increase in G_S of *L. styraciflua* following fertilization of eCO_2 plots in 2005 (Figure 6) represents the greatest departure from the $A_H - G_{SRef}$ relationship (Table 4), which would predict a 27% decrease in G_{SRef} during this year. In *P. taeda*, it may be that this effect of increased G_S with N_F is greatest in the lower canopy, as short-term porometry studies in 2005 did not detect such a decrease in G_S of foliage of the upper third of the canopy (Maier et al. 2008). Indeterminate species such as *L. styraciflua* may change leaf-specific conductivity by relatively rapid increases in leaf area, perhaps explaining the shorter duration of this effect in this species. Without more detailed data, however, such a transitory effect in either species cannot be confirmed.

Other structural and hydraulic effects on G_S

While we chose A_H as a representative structural characteristic for the trees in this study, we cannot conclude that the $A_H - G_{SRef}$ relationships are driven by hydraulic limitations alone. The changes in G_{SRef} that accompany changes in A_H could also result from a decrease in average leaf irradiance with increases in canopy A_L leading to a decrease in nitrogen

per unit leaf area and photosynthetic rate. However, as photosynthesis and nitrogen distributions do not precisely follow the distribution of light within forest canopies (Kull 2002), testing such a hypothesis would require more intensive measurements and analyses. Estimating light availability in a conifer-dominated canopy requires detailed modeling efforts (Kim et al. 2011), but represents a possible avenue for further investigation into the relative supply of water and light resources to the canopy between treatments and across years. We would note, however, that we did not observe clear relationships between A_L and any model parameters (data not shown), as we did for G_{SRef} and A_H (Figure 11).

As noted in the introduction, A_H is only an index of the scaling of the hydraulic supply, which varies along the pathway. It does not take into account scaling of root area, for example, which may show a different relationship to treatments than stem sapwood area (Ewers et al. 2000, Hacke et al. 2000, Sperry et al. 2002). The 26% increase in *P. taeda* A_L with eCO_2 over the 2005–08 study period presented here was accompanied by a 24–30% increase in stand fine root mass (Jackson et al. 2009), which are both proportional to the 22–30% increase in net primary productivity (McCarthy et al. 2010) in this species and suggest that differences in G_S of this species do not arise from changes in fine root-to-leaf-area ratio. There was an increase of 135% in the sapwood conductivity (k_Ψ, Eq. 1) of *P. taeda* coarse roots at maximum Ψ with eCO_2 (Domec et al. 2010), which should lead to increased water supply from the roots in the absence of changes in root-to-leaf-area ratios. Thus, the hydraulic supply from coarse roots may be one reason that G_{SRef} in the EC treatment is higher than predicted from changes in A_H alone (Table 2).

Differences in the ratio of outer to mean sap flux in *P. taeda* (Figure 8) would suggest differences between average k_Ψ (Eq. 1) at breast height in the combined (EF) treatment and that of the other treatments. A general trend of increases in this ratio with time in the other treatments may result from an increase in specific conductivity of sapwood with cambial age, as observed in *Pinus ponderosa* (Douglas ex C. Lawson) (Domec et al. 2005), as well as from a loss of functionality of older sapwood. It would seem more likely that the specific conductivity of newly developed xylem drops with fertilization in eCO_2 than the functional longevity of sapwood grown before fertilization increases, though either could lead to this result. In a longer-term experiment, this could lead to changes in the $A_H - G_{SRef}$ relationship of the EF treatment. Comparison of sapwood samples from plots of the original fertilization experiment begun in 1999 to those plots initially fertilized in 2005 may yield some insight into this possibility.

Modeling approach

While the general approach to modeling G_S as a series of interacting empirical functions to environmental drivers (Eq. 2) is over three decades old (Jarvis 1976), the hierarchical Bayes state-space approach we employ here differs significantly from most approaches used on such data sets. The most important feature of our approach is that it represents a consistent way to generate continuous estimates of E_L and G_S from hundreds of sap flux sensors over thousands of time steps (Figure 4). We believe that this approach is most useful for large-scale and/or long-term sap flux studies, where sensor replacement requires changes in sampling locations over time and gaps in data are unavoidable. By using a hierarchical structure that deals with data at the sensor level, the former issue is dealt with efficiently by the data model. The process of interest, canopy-averaged G_S, is dealt with in a state-space structure that deals with the latter issue and computes an uncertainty in this process that can be inform further modeling or experimental design efforts, such as constraining estimates of gross primary productivity (Schäfer et al. 2003, Kim et al. 2008). Proper quantification of uncertainty in a hierarchical structure can also assist experimenters in identifying which measurements contribute the most to uncertainty in processes of interest, informing future sampling designs to optimize the allocation of limited resources for monitoring networks (Clark et al. 2011).

Supplementary data

Supplementary data for this article are available at *Tree Physiology* Online.

Conflict of interest

None declared.

Funding

This research was supported by the Office of Science (BER) of US Department of Energy through Terrestrial Carbon Processes (TCP) program (FACE, DE-FG02-95ER62083), and by a BER Graduate Research Environmental Fellowship granted to the lead author.

References

Ainsworth EA, Long SP (2005) What have we learned from 15 years of free-air CO_2 enrichment (FACE)? A meta-analytic review of the responses of photosynthesis, canopy properties and plant production to rising CO_2. New Phytol 165:351–372.

Ainsworth EA, Rogers A (2007) The response of photosynthesis and stomatal conductance to rising [CO_2]: mechanisms and environmental interactions. Plant Cell Environ 30:258–270.

Bell DM (2011) Longterm approaches to assessing tree community responses to resource limitation and climate variation. Doctoral Dissertation, University Program in Ecology, Duke University, Durham, NC, USA, p 167. doi:10.1097/00000637-199510000-00004.

Buckley TN, Roberts DW (2005) How should leaf area, sapwood area and stomatal conductance vary with tree height to maximize growth? Tree Physiol 26:145.

Bush SE, Hultine KR, Sperry JS, Ehleringer JR (2010) Calibration of thermal dissipation sap flow probes for ring- and diffuse-porous trees. Tree Physiol 30:1545–1554.

Ceulemans R, Mousseau M (1994) Tansley Review No. 71: effects of elevated atmospheric CO_2 on woody plants. New Phytol 127:425–446.

Ceulemans R, Jiang XN, Shao BY (1995) Growth and physiology of one-year old poplar (*Populus*) under elevated atmospheric CO_2 levels. Ann Bot 75:609–617.

Clark JS, Agarwal P, Bell DM, Flikkema PG, Gelfand A, Nguyen X, Ward E, Yang J (2011) Inferential ecosystem models, from network data to prediction. Ecol Appl 21:1523–1536.

Curtis PS, Teeri JA (1992) Seasonal responses of leaf gas exchange to elevated carbon dioxide in *Populus grandidentata*. Can J For Res 22:1320–1325.

Domec JC, Pruyn ML, Gartner BL (2005) Axial and radial profiles in conductivities, water storage and native embolism in trunks of young and old-growth ponderosa pine trees. Plant Cell Environ 28:1103–1113.

Domec JC, Noormets A, King JS, Sun GE, McNulty SG, Gavazzi MJ, Boggs JL, Treasure EA (2009*a*) Decoupling the influence of leaf and root hydraulic conductances on stomatal conductance and its sensitivity to vapour pressure deficit as soil dries in a drained loblolly pine plantation. Plant Cell Environ 32:980–991.

Domec JC, Palmroth S, Ward E, Maier CA, Therezien M, Oren R (2009*b*) Acclimation of leaf hydraulic conductance and stomatal conductance of *Pinus taeda* (loblolly pine) to long-term growth in elevated CO_2 (free-air CO_2 enrichment) and N-fertilization. Plant Cell Environ 32:1500–1512.

Domec J-C, Schäfer KVR, Oren R, Kim HS, McCarthy HR (2010) Variable conductivity and embolism in roots and branches of four contrasting tree species and their impacts on whole-plant hydraulic performance under future atmospheric CO_2 concentration. Tree Physiol 30:1001–1015.

Drake JE, Raetz LM, Davis SC, DeLucia EH (2010) Hydraulic limitation not declining nitrogen availability causes the age-related photosynthetic decline in loblolly pine (*Pinus taeda* L.). Plant Cell Environ 33:1756–1766.

Eamus D, Jarvis PG (1989) The direct effects of increase in the global atmospheric CO_2 concentration on natural and commercial temperate trees and forests. In: Begon A, MacFadyen A (eds). Advances in ecological research. Academic Press, London, pp 1–55.

Ellsworth DS, Thomas R, Crous KY, Palmroth S, Ward E, Maier C, DeLucia E, Oren R (2011) Elevated CO_2 affects photosynthetic responses in canopy pine and subcanopy deciduous trees over 10 years: a synthesis from Duke FACE. Glob Change Biol 18:223–242.

Ewers BE, Oren R (2000) Analyses of assumptions and errors in the calculation of stomatal conductance from sap flux measurements. Tree Physiol 20:579.

Ewers BE, Oren R, Sperry JS (2000) Influence of nutrient versus water supply on hydraulic architecture and water balance in *Pinus taeda*. Plant Cell Environ 23:1055–1066.

Ewers BE, Oren R, Johnsen KH, Landsberg JJ (2001) Estimating maximum mean canopy stomatal conductance for use in models. Can J For Res 31:198–207.

Ford CR, McGuire MA, Mitchell RJ, Teskey RO (2004) Assessing variation in the radial profile of sap flux density in *Pinus* species and its effect on daily water use. Tree Physiol 24:241–249.

Gelfand AE, Smith AFM (1990) Sampling-based approaches to calculating marginal densities. J Am Stat Assoc 85:398–409.

Gough CM, Seiler JR, Johnsen KH, Sampson DA (2004) Seasonal photosynthesis in fertilized and nonfertilized loblolly pine. For Sci 50:1–9.

Granier A (1985) Une nouvelle methode pour la mesure du flux de seve brute dans le tronc des arbres. Ann For Sci 42:193–200.

Granier A (1987) Evaluation of transpiration in a Douglas-fir stand by means of sap flow measurements. Tree Physiol 3:309–320.

Gunderson CA, Wullschleger SD (1994) Photosynthetic acclimation in trees to rising atmospheric CO_2: a broader perspective. Photosynth Res 39:369–388.

Gunderson CA, Sholtis JD, Wullschleger SD, Tissue DT, Hanson PJ, Norby RJ (2002) Environmental and stomatal control of photosynthetic enhancement in the canopy of a sweetgum (*Liquidambar styraciflua* L.) plantation during 3 years of CO_2 enrichment. Plant Cell Environ 25:379–393.

Hacke UG, Sperry JS, Ewers BE, Ellsworth DS, Schafer KVR, Oren R (2000) Influence of soil porosity on water use in *Pinus taeda*. Oecologia 124:495–505.

Hendrey GR, Kimball BA (1994) The FACE program. Agric For Meteorol 70:3–14.

Hendrey GR, Ellsworth DS, Lewin KF, Nagy J (1999) A free-air enrichment system for exposing tall forest vegetation to elevated atmospheric CO_2. Glob Change Biol 5:293–309.

Herrick JD, Maherali H, Thomas RB (2004) Reduced stomatal conductance in sweetgum (*Liquidambar styraciflua*) sustained over long-term CO_2 enrichment. New Phytol 162:387–396.

Jackson RB, Cook CW, Pippen JS, Palmer SM (2009) Increased belowground biomass and soil CO_2 fluxes after a decade of carbon dioxide enrichment in a warm-temperate forest. Ecology 90:3352–3366.

Jarvis PG (1975) Water transfer in plants. In: de Vries DA, Afgan NG (eds) Heat and mass transfer in the environment of vegetation. Scripta Book Company, Washington, DC, pp 369–394.

Jarvis PG (1976) The interpretation of the variations in leaf water potential and stomatal conductance found in canopies in the field. Philos Trans R Soc Lond Ser B Biol Sci 593–610.

Kim HS, Oren R, Hinckley TM (2008) Actual and potential transpiration and carbon assimilation in an irrigated poplar plantation. Tree Physiol 28:559.

Kim H-S, Palmroth S, Therezien M, Stenberg P, Oren R (2011) Analysis of the sensitivity of absorbed light and incident light profile to various canopy architecture and stand conditions. Tree Physiol 31:30–47.

Kull O (2002) Acclimation of photosynthesis in canopies: models and limitations. Oecologia 133:267–279.

Lewin KF, Hendrey GR, Kolber Z (1992) Brookhaven National Laboratory free-air carbon dioxide enrichment facility. Crit Rev Plant Sci 11:135–141.

Loustau D, Domec JC, Bosc A (1998) Interpreting the variations in xylem sap flux density within the trunk of maritime pine (*Pinus pinaster* Ait.): application of a model for calculating water flows at tree and stand levels. Ann Sci For 55:29–46.

Lu P, Urban L, Zhao P (2004) Granier's thermal dissipation probe (TDP) method for measuring sap flow in trees: theory and practice. Acta Bot Sin 46:631–646.

Luo Y, Medlyn B, Hui D, Ellsworth D, Reynolds J, Katul G (2001) Gross primary productivity in Duke Forest: modeling synthesis of CO_2 experiment and eddy-flux data. Ecol Appl 11:239–252.

Mackay DS, Ewers BE, Loranty MM, Kruger EL, Samanta S (2012) Bayesian analysis of canopy transpiration models: a test of posterior parameter means against measurements. J Hydrol 432–433:75–83.

Maier CA, Palmroth S, Ward E (2008) Short-term effects of fertilization on photosynthesis and leaf morphology of field-grown loblolly pine following long-term exposure to elevated CO_2 concentration. Tree Physiol 28:597–606.

McCarthy HR, Oren R, Finzi AC, Johnsen KH (2006) Canopy leaf area constrains $[CO_2]$-induced enhancement of productivity and partitioning among aboveground carbon pools. Proc Natl Acad Sci USA 103:19356–19361.

McCarthy HR, Oren R, Finzi AC, Ellsworth DS, Kim H-S, Johnsen KH, Millar B (2007) Temporal dynamics and spatial variability in the enhancement of canopy leaf area under elevated atmospheric CO_2. Glob Change Biol 13:2479–2497.

McCarthy HR, Oren R, Johnsen KH, Gallet-Budynek A, Pritchard SG, Cook CW, LaDeau SL, Jackson RB, Finzi AC (2010) Re-assessment of plant carbon dynamics at the Duke free-air CO_2 enrichment site: interactions of atmospheric [CO_2] with nitrogen and water availability over stand development. New Phytol 185:514–528.

McDowell N, Barnard H, Bond B et al. (2002) The relationship between tree height and leaf area: sapwood area ratio. Oecologia 132:12–20.

Medlyn BE, Barton CVM, Broadmeadow MSJ et al. (2001) Stomatal conductance of forest species after long-term exposure to elevated CO_2 concentration: a synthesis. New Phytol 149:247–264.

Mencuccini M (2002) Hydraulic constraints in the functional scaling of trees. Tree Physiol 22:553.

Mencuccini M (2003) The ecological significance of long-distance water transport: short-term regulation, long-term acclimation and the hydraulic costs of stature across plant life forms. Plant Cell Environ 26:163–182.

Moore G, Bond B, Jones J, Meinzer F (2010) Thermal-dissipation sap flow sensors may not yield consistent sap-flux estimates over multiple years. Trees Struct Funct 24:165–174.

Mousseau M, Saugier B (1992) The direct effect of increased CO_2 on gas exchange and growth of forest tree species. J Exp Bot 43:1121–1130.

Murthy R, Dougherty PM, Zarnoch SJ, Allen HL (1996) Effects of carbon dioxide, fertilization, and irrigation on photosynthetic capacity of loblolly pine trees. Tree Physiol 16:537–546.

Norby RJ, Gunderson CA, Wullschleger SD, O'Neill EG, McCracken MK (1992) Productivity and compensatory responses of yellow-poplar trees in elevated CO_2. Nature 357:322–324.

Norby RJ, Wullschleger SD, Gunderson CA, Johnson DW, Ceulemans R (1999) Tree responses to rising CO_2 in field experiments: implications for the future forest. Plant Cell Environ 22:683–714.

Novick K, Oren R, Stoy P, Juang J-Y, Siqueira M, Katul G (2009) The relationship between reference canopy conductance and simplified hydraulic architecture. Adv Water Resour 32:809–819.

Oishi AC, Oren R, Stoy PC (2008) Estimating components of forest evapotranspiration: a footprint approach for scaling sap flux measurements. Agric For Meteorol 148:1719–1732.

Oishi AC, Oren R, Novick KA, Palmroth S, Katul GG (2010) Interannual invariability of forest evapotranspiration and its consequence to water flow downstream. Ecosystems 13:421–436.

Oren R, Phillips N, Katul G, Ewers BE, Pataki DE (1998) Scaling xylem sap flux and soil water balance and calculating variance: a method for partitioning water flux in forests. Ann Sci For 55:191–216.

Oren R, Sperry JS, Katul GG, Pataki DE, Ewers BE, Phillips N, Schafer KVR (1999) Survey and synthesis of intra- and interspecific variation in stomatal sensitivity to vapour pressure deficit. Plant Cell Environ 22:1515–1526.

Oren R, Ellsworth DS, Johnsen KH et al. (2001) Soil fertility limits carbon sequestration by forest ecosystems in a CO_2-enriched atmosphere. Nature 411:469–472.

Pataki DE, Oren R, Tissue DT (1998) Elevated carbon dioxide does not affect average canopy stomatal conductance of *Pinus taeda* L. Oecologia 117:47–52.

Pearcy RW, Schulze ED, Zimmermann R (1989) Measurement of transpiration and leaf conductance. In: Pearcy RW, Ehleringer JR, Mooney HA, Rundel PW (eds) Plant physiological ecology, field methods and instrumentation. Chapman & Hall, New York, pp 137–160.

Phillips N, Oren R (1998) A comparison of daily representations of canopy conductance based on two conditional time-averaging methods and the dependence of daily conductance on environmental factors. Ann Sci For 55:217–235.

Phillips N, Oren R, Zimmermann R (1996) Radial patterns of xylem sap flow in non-, diffuse- and ring-porous tree species. Plant Cell Environ 19:983–990.

Rayment MB, Loustau D, Jarvis PG (2000) Measuring and modeling conductances of black spruce at three organizational scales: shoot, branch and canopy. Tree Physiol 20:713–723.

Ritz C, Spiess AN (2008) qpcR: an R package for sigmoidal model selection in quantitative real-time polymerase chain reaction analysis. Bioinformatics 24:1549–1551.

Saxe H, Ellsworth DS, Heath J (1998) Tree and forest functioning in an enriched CO_2 atmosphere. New Phytol 139:395–436.

Schäfer KVR, Oren R, Tenhunen JD (2000) The effect of tree height on crown level stomatal conductance. Plant Cell Environ 23:365–375.

Schäfer KVR, Oren R, Lai CT, Katul GG (2002) Hydrologic balance in an intact temperate forest ecosystem under ambient and elevated atmospheric CO_2 concentration. Glob Change Biol 8:895–911.

Schäfer KVR, Oren R, Ellsworth DS, Lai CT, Herrick JD, Finzi AC, Richter DD, Katul GG (2003) Exposure to an enriched CO_2 atmosphere alters carbon assimilation and allocation in a pine forest ecosystem. Glob Change Biol 9:1378–1400.

Schwarz G (1978) Estimating the dimension of a model. Ann Stat 6:461–464.

Shinozaki K, Yoda K, Hozumi K, Kira T (1964) A quantitative analysis of plant form: the pipe model theory, 1. Jpn J Ecol 14:97–105.

Smith DM, Allen SJ (1996) Measurement of sap flow in plant stems. J Exp Bot 47:1833–1844.

Sperry JS, Hacke UG, Oren R, Comstock JP (2002) Water deficits and hydraulic limits to leaf water supply. Plant Cell Environ 25:251–263.

Steppe K, De Pauw DJW, Doody TM, Teskey RO (2010) A comparison of sap flux density using thermal dissipation, heat pulse velocity and heat field deformation methods. Agric For Meteorol 150:1046–1056.

Swanson RH (1972) Water transpired by trees is indicated by heat pulse velocity. Agric Meteorol 10:277–281.

Swanson RH, Whitfield DWA (1981) A numerical analysis of heat pulse velocity theory and practice. J Exp Bot 32:221.

Taneda H, Sperry JS (2008) A case-study of water transport in co-occurring ring- versus diffuse-porous trees: contrasts in water-status, conducting capacity, cavitation and vessel refilling. Tree Physiol 28:1641–1651.

Tateishi M, Kumagai TÄ, Utsumi Y, Umebayashi T, Shiiba Y, Inoue K, Kaji K, Cho K, Otsuki K (2008) Spatial variations in xylem sap flux density in evergreen oak trees with radial-porous wood: comparisons with anatomical observations. Trees Struct Funct 22:23–30.

Team RDC (2009) R: A language and environment for statistical computing. R Foundation for Statistical Computing, Vienna, Austria.

Thiec D, Dixon M, Loosveldt P, Garrec JP (1995) Seasonal and annual variations of phosphorus, calcium, potassium and manganese contents in different cross-sections of *Picea abies* (L.) Karst. needles and *Quercus rubra* L. leaves exposed to elevated CO_2. Trees Struct Funct 10:55–62.

Tyree MT, Ewers FW (1991) Tansley Review No. 34. The hydraulic architecture of trees and other woody plants. New Phytol 119:345–360.

Ward EJ, Bell DM, Clark JS, Oren R (2013). Hydraulic time constants for transpiration of loblolly pine at a free-air carbon dioxide enrichment site. Tree Physiology 33:123–134.

Waring RH, Schroeder PE, Oren R (1982) Application of the pipe model theory to predict canopy leaf area. Can J For Res 12:556–560.

Warren JM, Norby RJ, Wullschleger SD (2011) Elevated CO_2 enhances leaf senescence during extreme drought in a temperate forest. Tree Physiol 31:117–130.

Warton D, Ormerod J (2007) smatr: (Standardised) major axis estimation and testing routines. R package version 2.1.

Whitehead D (1998) Regulation of stomatal conductance and transpiration in forest canopies. Tree Physiol 18:633–644.

Whitehead D, Jarvis PG (1981) Coniferous forests and plantations. In: Kozlowski TT (ed.) Water deficits and plant growth. Academic Press, London, pp 49–152.

Whitehead D, Teskey RO (1995) Dynamic response of stomata to changing irradiance in loblolly pine (*Pinus taeda* L.). Tree Physiol 15:245–251.

Whitehead D, Edwards WRN, Jarvis PG (1984) Conducting sapwood area, foliage area, and permeability in mature trees of *Picea sitchensis* and *Pinus contorta*. Can J For Res 14:940–947.

Will RE, Teskey RO (1997) Effect of irradiance and vapour pressure deficit on stomatal response to CO_2 enrichment of four tree species. J Exp Bot 48:2095–2095.

Woodward FI (1990) Global change: translating plant ecophysiological responses to ecosystems. Trends Ecol Evol 5:308–311.

Wullschleger SD, Meinzer FC, Vertessy RA et al. (1998) A review of whole-plant water use studies in trees. Tree Physiol 18:499–512.

Wullschleger SD, Gunderson CA, Hanson PJ, Wilson KB, Norby RJ (2002) Sensitivity of stomatal and canopy conductance to elevated CO_2 concentration—interacting variables and perspectives of scale. New Phytol 153:485–496.

Wullschleger SD, Childs KW, King AW, Hanson PJ (2011) A model of heat transfer in sapwood and implications for sap flux density measurements using thermal dissipation probes. Tree Physiol 31:669–679.

Zak D, Pregitzer K, Curtis P, Teeri J, Fogel R, Randlett D (1993) Elevated atmospheric CO_2 and feedback between carbon and nitrogen cycles. Plant Soil 151:105–117.